JOURNAL OF MATERIALS SCIENCE 29 (1994) 1090–1096

Processing and properties of $Pb(Mg_{1/3}Nb_{2/3})O_3$–$PbZrO_3$–$PbTiO_3$ ceramic relaxors

M. VILLEGAS, J. R. JURADO, C. MOURE, P. DURAN
Instituto de Cerámica y Vidrio (CSIC), Electroceramics Department, 28500 Arganda del Rey, Madrid, Spain

The shrinkage phenomenon during the reaction-sintering of PMN–PZT from low-temperature pre-reacted $3PbO + MgNb_2O_6 + PZT$ powder mixtures has been studied. It was assumed that the pre-reaction treatment leads to the formation of a pyrochlore phase containing very active MgO small particles, and that the strong shrinkage occurring up to 800 °C took place by the diffusion of Mg^{2+} cations into the pyrochlore phase particles, thus controlling the reaction-sintering shrinkage phenomenon. Above that temperature the densification was enhanced by a liquid-phase sintering process. The ceramics sintered at 1050 °C for 2 h showed ~96% of the theoretical density, and the dielectric constant of such a sintered ceramic showed a maximum value of 17 000 at 1 kHz. It was also found that the dielectric constant decreased with increasing grain size. Although the role of PZT in enhancing the dielectric constant of otherwise low-purity PMN ceramics is not clear, the increase in K is assumed to be a solid-solution effect. The presence of impurities and the PbO stoichiometry could be influencing the not too high dielectric constant value of PMN–PZT ceramics.

1. Introduction

Lead magnesium niobate, $Pb(Mg_{1/3}Nb_{2/3})O_3$ (PMN), is a good candidate to fabricate multilayer ceramic capacitors in view of its high dielectric constant, low dissipation factor and high volumetric efficiency. However, pure PMN is a ceramic material presenting many problems related to both the synthesis and the sintering. Its synthesis has been studied extensively by conventional ceramic pathways [1–4] and by using precursor processes [5–7]. The main conclusion was the difficulty of obtaining a perovskite PMN single phase at the end of the synthesis process. The presence of a pyrochlore phase in variable amounts along with the perovskite phase was a common finding in all cases. Such a pyrochlore phase has a significant influence on the dielectric properties of the PMN ceramics [8, 9]. Several perovskite structure additives which enhance both the amount of perovskite phase and the stability have also been studied [10, 11]. The formation of a PMN solid solution with a higher skeleton perovskite ionicity seems to be the reason for such an enhancement [10].

Concerning the sintering process, it is well known that a good control of PbO content is extremely important not only to inhibit pyrochlore phase formation but also to enhance the densification through liquid-phase sintering [12]. However, the presence of free PbO in the grain boundary can have a detrimental effect on both dielectric and mechanical properties. Therefore any procedure tending to minimize the volatilization of PbO would have a favourable effect on the performance of sintered PMN ceramics.

One of the objectives of the present work was to study the possibility of directly obtaining sintered PMN ceramics from a $3PbO + MgNb_2O_6 + PZT$ (lead zirconate titanate) low-temperature pre-reacted powder mixture, avoiding in such a way the PMN powder synthesis step. On the other hand, the influence of such a powder processing on the microstructure and dielectric properties of the reaction-sintered PMN–PZT bodies will also be studied.

2. Experimental procedure

The required 0.9 $Pb(Mg_{1/3}Nb_{2/3})O_3$–0.1 $Pb(Zr_{0.40}Ti_{0.60})O_3$ composition was prepared by mixing weighed raw materials of PbO (99.8% purity), $MgNb_2O_6$ and PZT. The columbite precursor ($MgNb_2O_6$) was obtained from the reaction of MgO with Nb_2O_5 powders at 1000 °C for a short time, and the PZT additive was prepared by coprecipitating the Ti^{4+} and Zr^{4+} hydroxides with a 6N-NH_4OH solution dropped into a PbO powder dispersion containing the above cations. After filtering and drying the powder was calcined at 500 °C for several hours, and the resulting oxide (PZT), having a specific surface area of $20\,m^2\,g^{-1}$, was mixed with PbO and $MgNb_2O_6$, attrition-milled for 2 h and dried. One part of the powder was pre-reacted at 500 to 600 °C for a short time. Both the pre-reacted (PR) and the unpre-reacted (UPR) powders were attrition-milled again for 2 h, granulated, isopressed at 200 MPa and sintered at 950 to 1200 °C for 4 h in air. The preparation process is shown in Fig. 1.

0022–2461

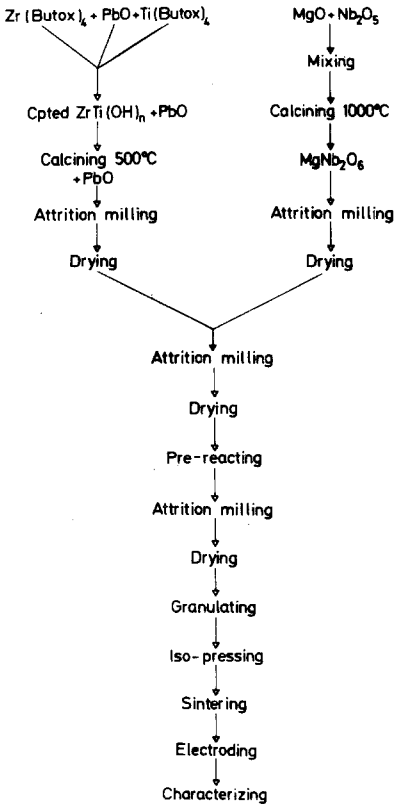

Figure 1 Schematic flow diagram for firing process of the PMN–PZT ceramics.

The powders were characterized by measuring both the specific surface area (BET) and the particle size (Sedigraph). Thermal expansion behaviour was studied on compacted samples by means of a dilatometer (Adamel Lhomargy DI-24) at a heating rate of 5 °C min^{-1} in the temperature range of 25 to 800 °C. Sintered density was measured by the Archimedes method with water. Microstructures of both the green bodies and the sintered ones were studied by scanning electron microscopy (SEM: Zeiss DM-950).

Measurements of dielectric constant and dissipation factor were carried out on sintered discs painted on both sides with silver paste. The dielectric constant and dielectric losses were studied as a function of the frequency in the range of 1 to 100 kHz by means of an impedance analyser (HP 4192A LF).

3. Results

Scanning electron micrographs of the attrition-milled powders before and after pre-reacting are shown in Fig. 2(a) and (b). In the first case the powder was constituted by small and soft agglomerates in which the primary particle size was less than 500 nm and the specific surface area was about 6 $m^2 g^{-1}$. After pre-reacting the powder morphology was strongly changed, but both the average particle size and the specific surface area were not appreciably shifted, 300 nm and 4 $m^2 g^{-1}$ as measured by SEM and BET, respectively.

Fig. 3a shows the granulated PR powder which was formed of almost spherical granules with sizes ranging from 10 to 100 μm, and Fig. 3b shows an SEM micrograph of the fracture surface of the compacted

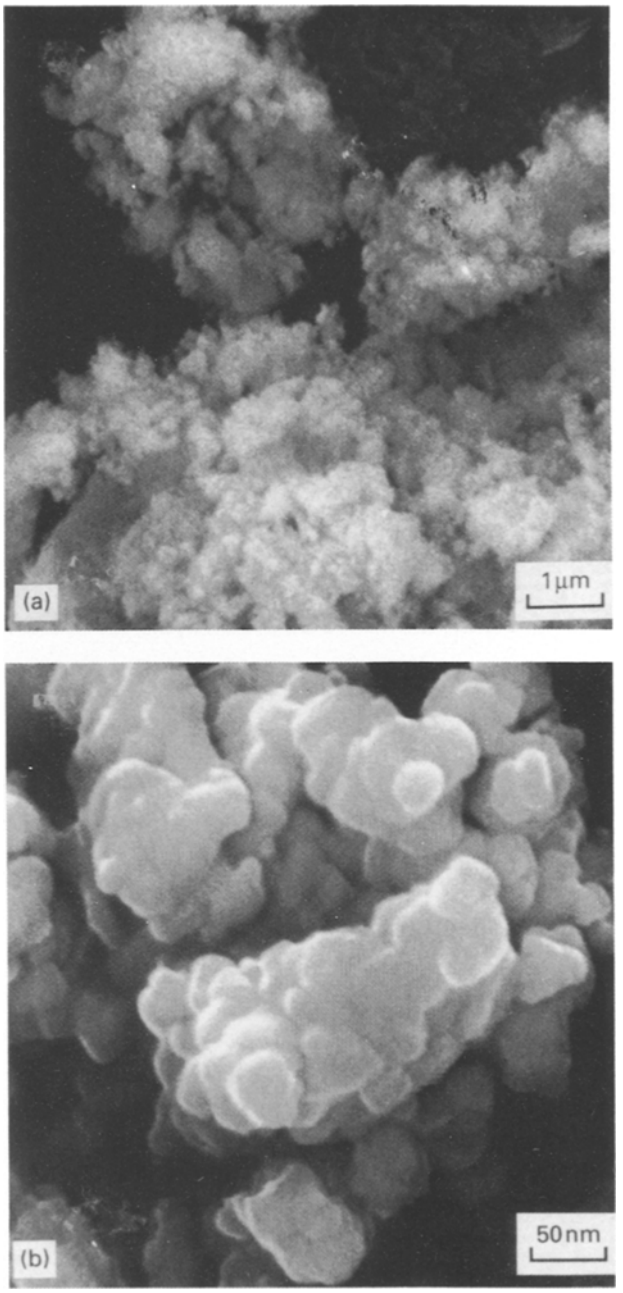

Figure 2 SEM of (a) UPR and (b) PR PMN–PZT powders.

green body (~ 45% theoretical density). Some strong agglomerates survived after isopressing, and were present as heterogeneities in the green microstructure.

The shrinkage and shrinkage rate curves for the PR compacted powder are shown in Fig. 4. For comparison the shrinkage curve obtained for UPR compact powder is also shown in the same figure. The shrinkage curve for the PR compacted powder presents two main peaks at 630 and 780 °C and the shrinkage rate curve shows, correspondingly, two others at 580 and 740 °C. In the same way the shrinkage for the UPR compacted powder also presents two peaks but the shrinkage behaviour was quite different.

The isothermal sintering of PR compacted samples and the weight losses are shown in Fig. 5. As can be seen, a rapid densification took place up to 1100 °C and then the density (~ 96% of the theoretical density) remained almost constant or slightly diminished

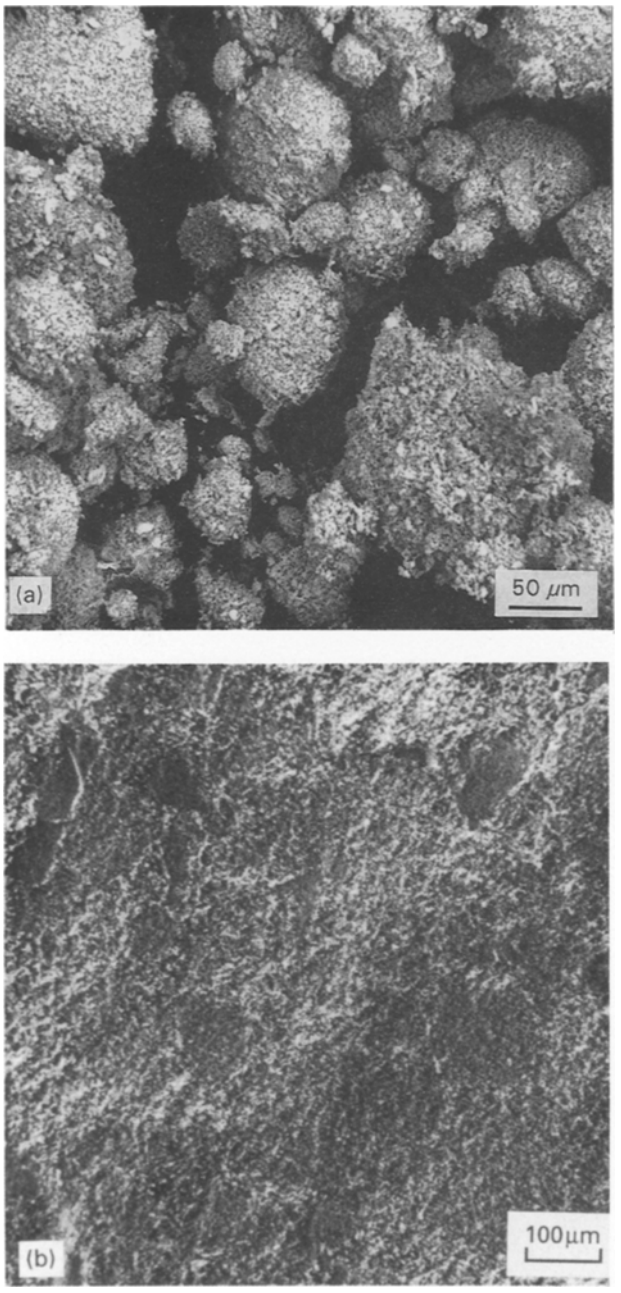

Figure 3 SEM of (a) granulated PR powder and (b) fracture surface of compacted green body.

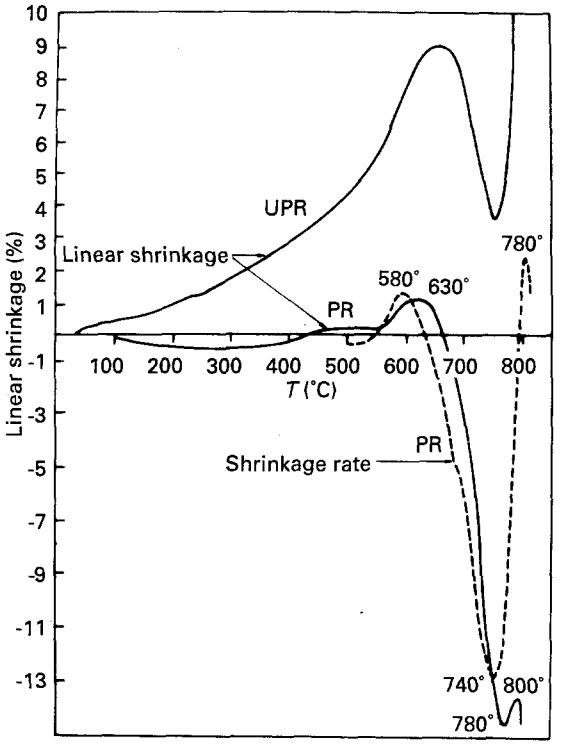

Figure 4 Shrinkage and shrinkage rate curves of UPR and PR compacted powders.

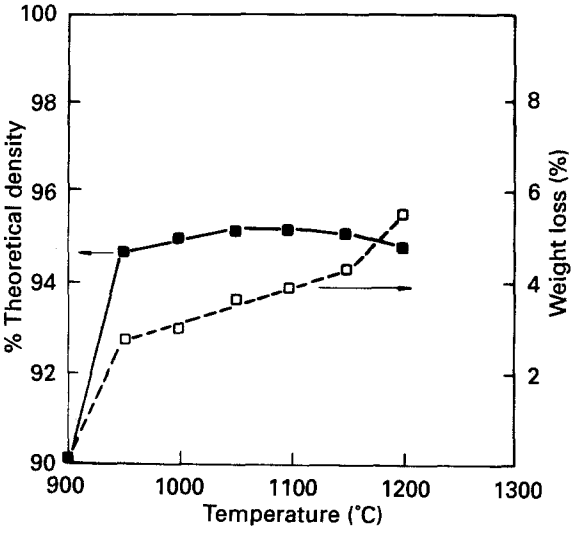

Figure 5 Isothermal sintering of PR compacted samples and PbO losses: (■) percentage theoretical density, (□) weight loss.

with increasing sintering temperature. The corresponding weight loss data showed that this increased with sintering temperature. By comparing the above two experiments it could be assumed that the slight decrease in density above 1000–1050 °C was related to the higher PbO loss from the samples in that temperature interval which generated an increase in porosity. The sintering density of the UPR compacted samples was never higher than 82% of the theoretical density.

Fig. 6 shows the lattice parameter variation for the sintering temperature range studied; no appreciable changes were found, indicating an extremely small compositional fluctuation after sintering. It must be noted that the PR and UPR compacted samples were perovskite PMN single phase at the end of the sintering process.

Scanning electron micrographs of PR and UPR fracture surface samples sintered at 1050 °C are shown in Fig. 7a and b. One can observe the extremely porous microstructure of the UPR sintered sample (~ 80% theoretical density) but there is also a uniform grain size of about 4 μm, with different grain morphologies among them as expected from a not well sintered material. In contrast the PR sintered samples show a microstructure with a mixture of intergranular and transgranular fracture as a consequence of the presence of some free PbO in the grain boundaries. An average grain size of about 7 μm could be measured at that sintering temperature, and some

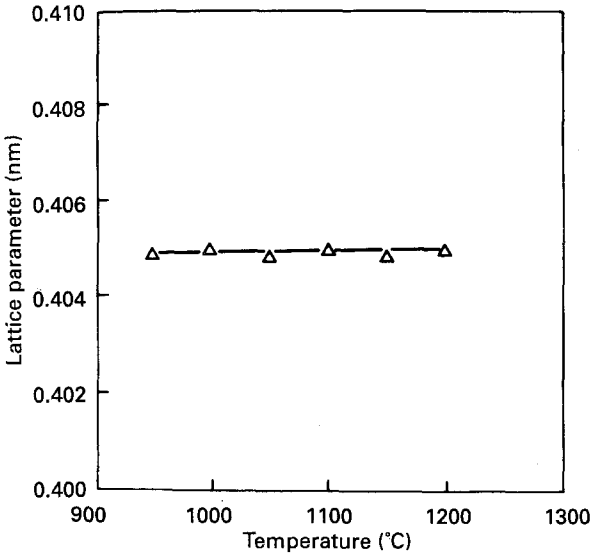

Figure 6 Lattice parameter variation of PR sintered samples as a function of sintering temperature.

pores in the interior of the grains can also be observed as a consequence of a grain growth rate faster than that of pore; migration toward the grain boundaries. Fig. 7c shows the microstructure of a PR compacted sample sintered at 1150 °C in which no PbO excess was present, showing a typical intergranular fracture surface. Fig. 8 shows the grain growth process in the temperature interval studied.

Fig. 9a and b show the variation of dielectric constant and dielectric losses with temperature and frequency, respectively, and it can be seen that the PR ceramic sintered at 1050 °C displays frequency-dispersive behaviour typical of ferroelectric relaxors. The transition between ferroelectric and paraelectric phases is broad and shows a maximum value of dielectric constant at 40 °C at 1 kHz and 45 °C at 100 kHz. In the same way the dielectric constant maxima were displaced from 13000 at 100 kHz to about 17000 at 1 kHz. PMN sintered ceramics without PZT addition had a peak dielectric constant of only 6000.

4. Discussion

The results above described have shown that it is possible to directly fabricate PMN–PZT dense bodies from a low-temperature (500 to 600 °C) pre-reacted $3PbO + MgNb_2O_6 + PZT$ powder mixture. The powder morphology and its small particle size favoured the rapid reaction of the above powder mixture in a short time at low temperature, leading to a pre-reacted powder formed by an intermediate pyrochlore phase containing very active MgO particles [13], with a sintering behaviour totally different to that of an un-pre-reacted powder mixture as evidenced by the shrinkage and shrinkage rate curves of the compacted samples (see Fig. 4). It seems that the low-temperature pre-reacting step contributed to eliminating the strong thermal expansion produced during the reaction of PbO with the columbite

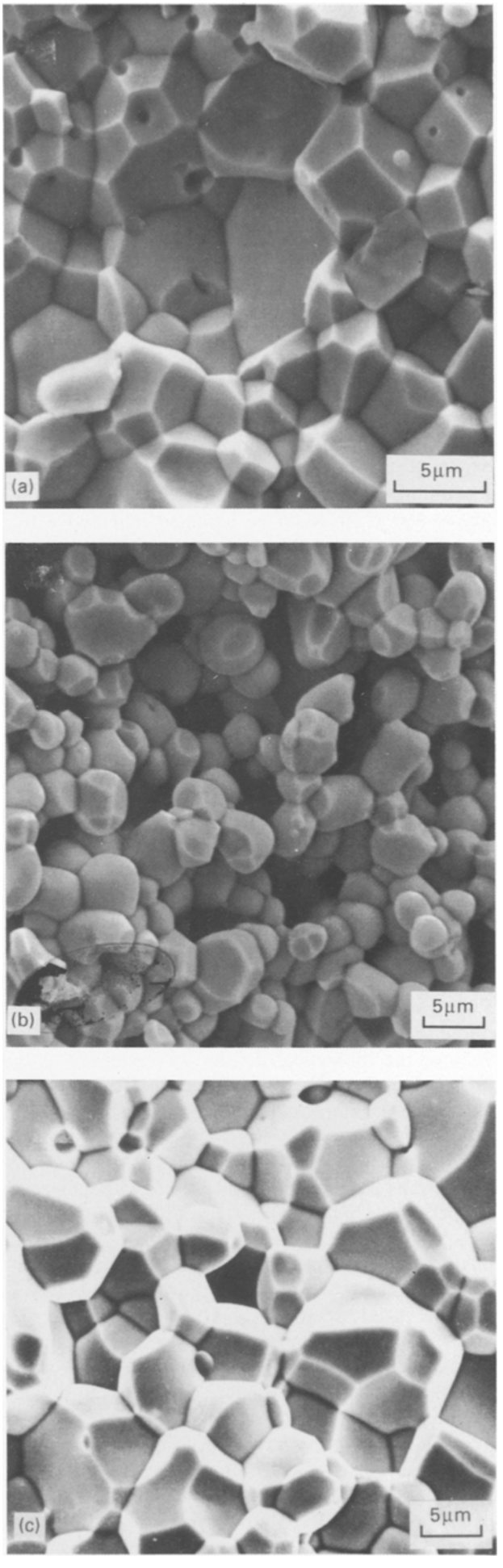

Figure 7 SEM of (a) PR and (b) UPR samples reaction-sintered at 1050 °C, and (c) PR sample reaction-sintered at 1150 °C.

($MgNb_2O_6$). In such a way, the densification process takes place with a strong shrinkage (~ 17%) of the compacted sample in the narrow temperature range of 630 to 780 °C, and a density as high as 90% of the theoretical density was achieved. The maximum of the densification rate took place at 740 °C, which is in agreement with the beginning of the transformation temperature of the pyrochlore phase to PMN perovskite [13]. These results suggest that the mechanism of the shrinkage phenomenon may be related to the solid-state diffusion of Mg^{2+} cations into the pyrochlore phase during its reaction to PMN and, if this is so, then such a mechanism was favoured by the small particle sizes of the pyrochlore and MgO in the compact. Thus it is reasonable to suggest that the Mg^{2+} is the controlling diffusing species for the shrinkage phenomenon. Therefore it is proposed that the reaction-sintering shrinkage mechanism is controlled by Mg^{2+} in the pyrochlore phase particles.

Although the shrinkage curve was not studied above 800 °C, it could be assumed that above that temperature the densification process takes place with the formation of a liquid phase which enhances the final density of the sintered bodies [14]. The presence of excess PbO to promote liquid-phase sintering would increase the magnitude of the shrinkage effect by an easier particle rearrangement. The increasing shrinkage rate above 780 °C supported such an assumption (see Fig. 4).

Isothermal sintering in air in the 900 to 1200 °C temperature interval corroborated the above results, and thus at a temperature as low as 950 °C the density was as high as 95% of the theoretical density as a consequence of PbO liquid-phase formation just below 900 °C (the melting point of PbO is 880 °C). Above that temperature the PbO activity could be considerable and the densification process is strongly influenced by PbO volatilization (see Fig. 5). Although the PbO liquid phase can aid densification, PbO loss generated an additional porosity and produced the opposite effect. In such a way no more than 96% of the theoretical density was achieved at the higher sintering temperature. Therefore the results in Fig. 5 are a compromise between densification and PbO losses.

The grain growth process in the PMN–PZT ceramics runs parallel to the PbO losses with increasing temperature. Up to 1100 °C the grain size rapidly grew as a consequence of the presence of a PbO liquid phase. At that temperature the PbO excess was completely lost and then the grain growth process ceased (see Fig. 8). Although above 1100 °C more PbO was lost, PbO coming from the PMN structure originated the subsequent small fluctuation in the composition and led to an inhomogeneous microstructure. This assumption was corroborated by studying the morphology of some fracture surfaces as shown in Fig. 10a, in which the various phases seem to exist. Such an SEM micrograph shows many round solid particles embedded in a liquid matrix. The EDS analysis of the round particles, as shown in Fig. 10b, revealed that the solid phases contained mainly Pb^{2+} and Nb^{5+} with very little Mg^{2+} and some Ti^{4+}. Zr^{4+}

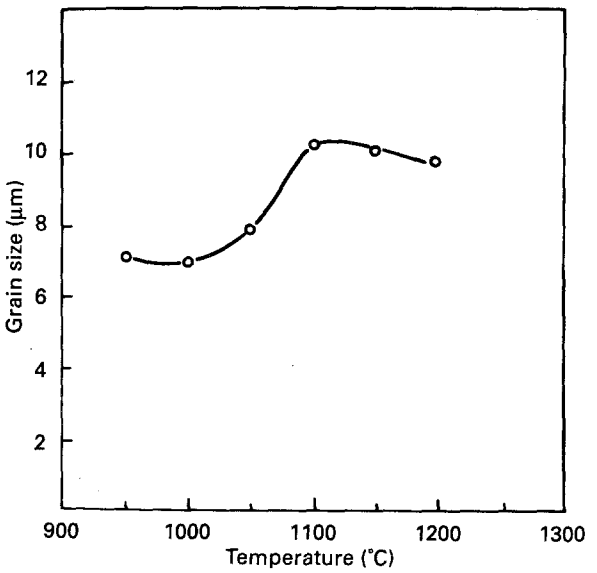

Figure 8 Grain growth as a function of sintering temperature.

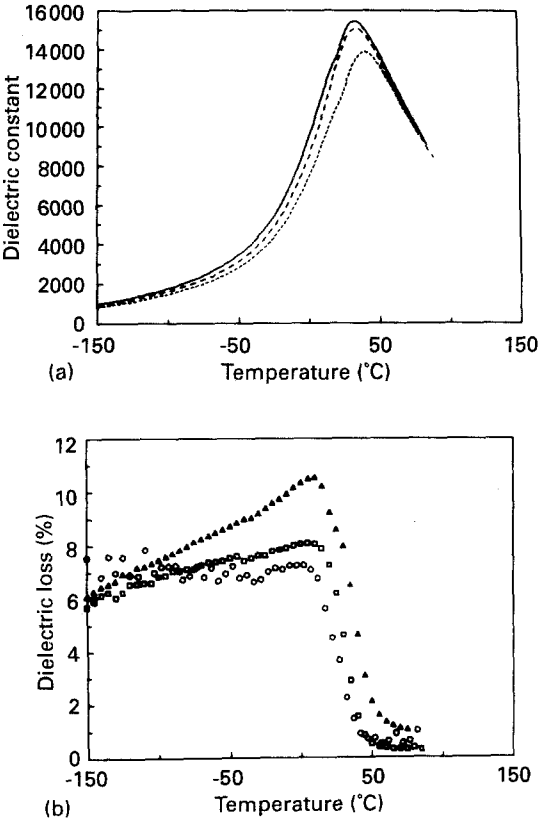

Figure 9 (a) Dielectric constant and (b) dielectric loss of PMN–PZT ceramic sintered for 4 h at 1050 °C, as a function of temperature and frequency: (○, ——) 1 kHz, (□, – – –) 10 kHz, (△, . . .) 100 kHz.

was not detected. The surrounding liquid was found to be predominantly constituted by Pb^{2+}, Si^{4+} and Na^{+}. These last two ions are due to the presence of impurities in the starting raw materials. A similar phenomenon was observed by Guha *et al.* [14] at a higher temperature, and was attributed to PbO loss from the sample surface as a consequence of prolonged high-temperature sintering.

It seems clear from Fig. 9 that the values of the pure PMN dielectric constant maxima are increased by the

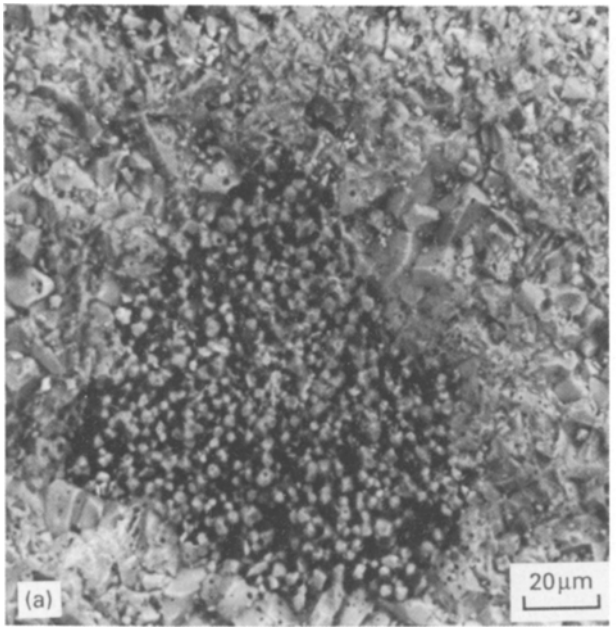

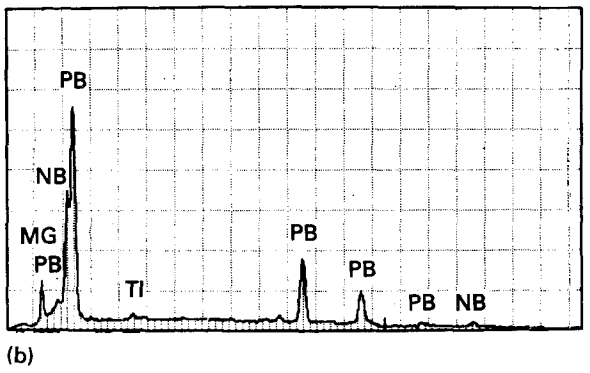

Figure 10 (a) SEM showing surface heterogeneity after sintering at 1050 °C and (b) EDS analysis.

addition of 10 mol% PZT and the corresponding tanδ values are decreased. In the same way, PZT addition increased the frequency dispersion of the dielectric constant maxima, and thus the temperature difference between 1 and 100 kHz dielectric constant maxima was 12 °C for PMN with 10 mol% PZT and 5 °C for pure PMN [15].

One of the most important results of the present work was the grain size dependence of the dielectric constant of PMN–PZT ceramics. In such a way a value of 17 000 was measured at the Curie temperature when the grain size was 7 μm, and 11 000 for a grain size of 10 μm. This result is in contrast with that reported by Swartz *et al.* [16] for which an increase of the dielectric constant with increasing grain size was found. On the other hand, Okazaki and Nagata [17] found in fine-grained PZT that at the Curie temperature the dielectric constant decreased with increasing grain size, and by comparison those results could be contrasted with the grain size dependence of dielectric constant in $BaTiO_3$ ceramics [18]. In these last two cases such a behaviour was attributed to a clamping of domain walls phenomenon and to internal stresses generated at the grain boundaries, respectively. However, Swartz *et al.* [16] suggested as more important

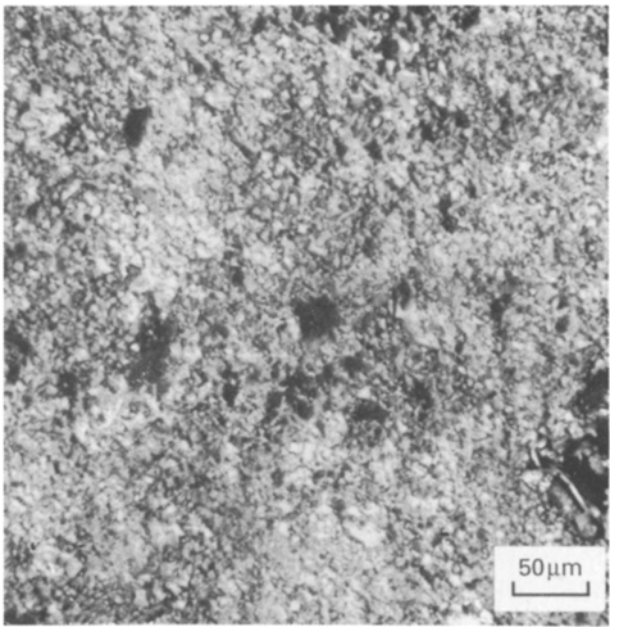

Figure 11 SEM of surface microstructure in PMN–PZT ceramics showing isolated second-phase areas.

the influence of the grain boundary, contrary to the results here reported. In our case it is believed that in the absence of a second phase such as the pyrochlore one with a low permittivity, the role of PbO excess in the sintered sample is crucial. From Fig. 7 it can be seen that during the earlier stages of sintering a high content of free PbO is present in the samples, but such an excess is rapidly lost as the sintering temperature is increased. At 1050 °C the PbO excess in the sintered samples was about 0.8 wt % and the density 96% of the theoretical one. At 1150 °C a PbO defect of about 1 wt % and 95% of theoretical density was found. Therefore it is assumed that in the first case the sample is saturated with PbO homogeneously distributed in the grains and, in such a way, the dielectric constant was improved. PMN ceramics containing up to 6 wt% PbO excess with improved dielectric properties were also reported by Lejeune and Boilot [12], but no satisfactory explanation could be offered for such a behaviour.

Although the results described above showed evidence for an enhancement of the dielectric constant in PMN ceramics containing 10 mol% PZT, the K values were never higher than 17 000 in the most favourable case, and this is very far from that measured in PMN single crystals ($\geqslant 20\,000$) [19]. Although many other parameters like density, grain size and stoichiometry could influence the dielectric constant, it seems reasonable to think that the impurity level, its nature and its distribution could also have an important role in decreasing the dielectric constant. The presence of a glassy phase (other than the liquid PbO) with a very low dielectric constant, if not uniformly distributed, could also have a strong influence on the dielectric constant of PMN–PZT ceramics. In that connection Fig. 11 shows the surface microstructure of a PMN–PZT sample sintered at 1050 °C in

which isolated large second-phase grains were observed. A very precise chemical analysis of those isolated grains, now in progress, could help to elucidate their influence on the dielectric properties of PMN–PZT ceramics. Chen and Harmer [20] stated that a well-distributed pyrochlore phase could not be the only factor in decreasing the dielectric constant. On the other hand Gorton *et al.* [21] reported that SiO_2 and/or ZrO_2 additions in concentration as low as 0.2 wt % could decrease the dielectric constant of pure PMN from 20 000 to 7 000. If this is so then it could be assumed that, in the absence of a pyrochlore phase detectable by X-ray diffraction, other factors such as non-uniform microstructure, stoichiometry problems and even the lattice impurities could be playing an important role in lowering the dielectric constant of PMN ceramics containing 10 mol % of PZT. A deeper study of the microstructural development, impurity distribution, chemical analysis and amounts of second phases present could help to elucidate it.

5. Conclusions

The shrinkage phenomenon during the reaction-sintering of PMN–PZT from a low-temperature pre-reacted $3PbO + MgNb_2O_6 + PZT$ powder mixture was studied. The small particle sizes of the constituents favoured rapid reaction between them, leading to an intermediate pyrochlore phase containing very active MgO particles homogeneously distributed. It is believed that, below the melting point of PbO, Mg^{2+} cations are the controlling diffusion species for the reaction-sintering shrinkage phenomenon. At higher temperatures the densification is enhanced by the formation of a PbO liquid phase. Addition of PZT stabilized the perovskite phase by means of PMN–PZT solid-solution formation. Although the dielectric properties of PMN–PZT ceramics were better than those of the corresponding undoped PMN ones, the presence of impurities and free PbO could be the cause for lowering the dielectric constant of the PMN–PZT ceramics studied here.

Acknowledgement

This research was supported by the Spanish Comisión Interministerial de Ciencia y Tecnología (CICYT) Mat-91-597.

References

1. G. A. SMOLENSKII and A. I. AGRANOVSKAYA, *Sov. Phys. Tech. Phys.* **3** (1958) 1380.
2. S. L. SWARTZ and T. R. SHROUT, *Mater. Res. Bull* **17** (1982) 1245.
3. M. LEJEUNE and J. P. BOILOT, *Ceram. Int.* **8** (1982) 99.
4. T. R. SHROUT and A. HALLIYAL, *Amer. Ceram. Soc. Bull.* **66** (1987) 704.
5. H. U. ANDERSON, M. J. PENELL and J. P. GUHA, *Adv. Ceram.* **21** (1987) 91.
6. P. RAVINDRANATHAN, S. KOMARNENI, A. S. BHALLA, R. ROY and L. E. CROSS, in "Ceramic Transactions", Vol. 1 (American Ceramic Society Inc., Westerville, Ohio, USA, 1988) p. 182.
7. F. CHAPUT, J. P. BOILOT, M. LEJEUNE, R. PAPIERNIK and L. H. PFALZGRAF, *J. Amer. Ceram. Soc.* **72** (1989) 1355.
8. K. FURUKAWA, S. FUJIWARA and T. OGASAWARA, in Proceedings of Japan–US Study Seminar on Dielectric and Piezoelectric Ceramics (1982) p. T-4.
9. J. CHEN, A. GORTON, H. M. CHAN and M. P. HARMER, *J. Amer. Ceram. Soc.* **69** (1986) C-303.
10. J. R. BELSIK, A. HALLIYAL, U. KUMAR and R. E. NEWNHAM, *Amer. Ceram. Soc. Bull.* **66** (1987) 664.
11. S. Y. CHEN, S. Y. CHENG, and C. M. WANG, *J. Amer. Ceram. Soc.* **74** (1991) 400.
12. M. LEJEUNE and J. P. BOILOT, *Amer. Ceram. Soc. Bull.* **64** (1986) 679.
13. M. VILLEGAS, J. R. JURADO, C. MOURE, and P. DURAN, *J. Mater. Sci.* in press.
14. J. P. GUHA, D. J. HONG and H. U. ANDERSON, *J. Amer. Ceram. Soc.* **71** (1988) C-152.
15. M. VILLEGAS, PhD thesis, Antonomous University, Madrid (1993).
16. S. L. SWARTZ, T. R. SHROUT, W. A. SCHULZE and L. E. CROSS, *J. Amer. Ceram. Soc.* **67** (1984) 311.
17. K. OKAZAKI and K. NAGATA, *J. Soc. Mater. Sci. Jpn* **41** (1972) 404.
18. W. R. BUESSEM, L. E. CROSS and A. K. GOSWAMI, *J. Amer. Ceram. Soc.* **49** (1966) 33.
19. V. A. BOKOV and I. E. MYLNIKOVA, *Sov. Phys. Solid State* **3** (1961) 613.
20. J. CHEN and M. P. HARMER, *J. Amer. Ceram. Soc.* **73** (1990) 68.
21. A. J. GORTON, C. M. SUNG, H. M. CHAN, D. M. SMYTH and M. P. HARMER, in "Ceramic Transactions", Vol. 8 American Ceramic Society Inc., Westerville, Ohio, USA, (1990) p. 116.

Received 29 July
and accepted 26 August 1993